Different levels of the neuronal nitric oxide synthase isoform modulate the rate of osteoclastic differentiation of TIB-71 and CRL-2278 RAW 264.7 murine cell clones

ARTICLE *in* THE ANATOMICAL RECORD PART A DISCOVERIES IN MOLECULAR CELLULAR AND EVOLUTIONARY BIOLOGY · OCTOBER 2005

DOI: 10.1002/ar.a.20239 · Source: PubMed

Different Levels of the Neuronal Nitric Oxide Synthase Isoform Modulate the Rate of Osteoclastic Differentiation of TIB-71 and CRL-2278 RAW 264.7 Murine Cell Clones

VANESSA NICOLIN,[1]* CRISTINA PONTI,[1] PAOLA NARDUCCI,[1] VITTORIO GRILL,[1] ROBERTA BORTUL,[1] MARINA ZWEYER,[1] MAURO VACCAREZZA,[2] AND GIORGIO ZAULI[1]

[1]Department of Normal Human Morphology, University of Trieste, Trieste, Italy
[2]Department of Health and Motor Sciences, University of Cassino, Cassino, Frosinone, Italy.

ABSTRACT

It has been clearly established that osteoclasts, which play a crucial role in bone resorption, differentiate from hematopoietic cells belonging to the monocyte/macrophage lineage in the presence of macrophage-colony stimulating factor (M-CSF) and receptor activator of NF-κB ligand (RANKL). We have here investigated the M-CSF- and RANKL-induced osteoclastic differentiation of two distinct clones of the murine monocytic/macrophagic RAW 264.7 cell line, known as TIB-71 and CRL-2278, the latter cell clone being defective for the expression of the inducible nitric oxide synthase isoform in response to interferon-γ or lipopolysaccharide. CRL-2278 cells demonstrated a more rapid osteoclastic differentiation than TIB-71 cells, as documented by morphology, tartrate-resistant acid phosphatase positivity, and bone resorption activity. The enhanced osteoclastic differentiation of CRL-2278 was accompanied by a higher rate of cells in the S/G2-M phases of cell cycle as compared to TIB-71. The analysis of nitric oxide synthase (NOS) isoforms clearly demonstrated that only neuronal NOS was detectable at high levels in CRL-2278 but not in TIB cells under all tested conditions. Moreover, the broad inhibitor of NOS activity L-NAME significantly inhibited osteoclastic differentiation of CRL-2278 cells. Altogether, these results demonstrate that a basal constitutive neuronal NOS activity positively affects the RANKL/M-CSF-related osteoclastic differentiation.

Key words: RAW 264.7; neuronal nitric oxide synthase; osteoclastogenesis; tartrate-resistant acid phosphatase

Bone represents a connective tissue evolving dinamically in order to keep a fine-tuned balance between locomotion mechanical integrity and mineral homeostasis control (Bab and Einthorn, 1994). Mineralized bone undergoes a continuous remodeling mediated by opposite biological phenomena: the production of new bone by osteoblasts balanced by bone resorption induced through osteoclasts modeling action. Osteoclasts are tissue-specific macrophage polykaryons achieved by the differentiation of cells belonging to the monocyte/macrophage lineage (Boyle et al., 2003). This differentiation is mainly regulated by two factors: macrophage-colony stimulating factor (M-CSF) and receptor activator of NF-κB ligand (RANKL), where M-CSF acts predominantly as a survival factor while RANKL is essential particularly for inducing terminal osteoclastic differentiation (Boyle et al., 2003). In

Grant sponsor: MIUR-FIRB 2001; Grant number: RBNE01SP72.

The first two authors contributed equally to this work.

*Correspondence to: Vanessa Nicolin, Department of Normal Human Morphology, University of Trieste, Via Manzoni 16, 34138 Trieste, Italy. Fax: 39-040-5586016. E-mail: nicolin@units.it

Received 6 April 2005; Accepted 1 July 2005

DOI 10.1002/ar.a.20239

Published online 2 September 2005 in Wiley InterScience (www.interscience.wiley.com).

addition to M-CSF and RANKL, osteoclastogenesis is also positively affected by inflammatory cytokines, such as IL-1β and TNF-α (Lee et al., 2001), while other cytokines, such as interferon-γ, IL-18, and TRAIL, block osteoclastic differentiation (Zauli et al., 2004).

Studies of the biological function of the RANK/RANKL interaction demonstrate that RANKL is essential to elicit osteoclast development. These observations are reinforced by osteoclast development inhibition by osteoprotegerin (OPG), a soluble RANKL-binding protein inhibiting RANK/RANKL complex formation. In osteoclasts, RANK/RANKL complex is able to recruit some adaptor proteins such as TRAF-6, TAB-2, IRAK 1–3 and, Src, which activate Akt, AP-1, and NF-κB (Ye et al., 2002). These transcription factors are involved in osteoclast cell differentiation and survival and play a pivotal role in the induction of bone remodeling. The pivotal role of the RANKL/RANK/OPG signaling pathways in regulating bone metabolism is reinforced by recent findings, evidencing that genetic mutations, activating RANK or inhibiting RANKL binding properties of OPG in humans, are associated with familiar forms of hyperphosphatasia and bone abnormalities (Cundy et al., 2002). Activating mutations in exon 1 of TNFRSF11A, the gene encoding RANK, have been found to be associated with osteolytic and nonosteolytic forms of hyperphosphatasia. Expansile skeletal hyperphosphatasia and familiar expansile osteolysis are allelic bone diseases caused by specific duplications in exon 1 of TNFRSF11A (Walsh and Choi, 2003). These duplications lengthen the signal peptide of RANK and seem likely to increase its biological activity by sequestering the receptor intracellularly and therefore causing excessive signaling through NF-κB (Liu et al., 2004).

Recently, several observations suggested that also the short-lived radical gas nitric oxide (NO) is tightly involved in the regulation of bone turnover. NO is generated from L-arginine by nitric oxyde synthase (NOS) isoenzymes. Three isoforms were described: a neuronal form (type I; nNOS), an endothelial form (type III; eNOS), and an inducible form (type II; iNOS). The eNOS and nNOS are constitutively expressed isoforms that yield to a rapid low output of NO, whereas iNOS is generally activated by cytokines and produce persistent high amounts of NO. Previous studies have evidenced contrasting and sometimes opposite effects of NO on osteoclastic bone resorption (Lowik et al., 1994; Brandi et al., 1995; Ralston et al., 1995; van't Hof and Ralston, 1997). On these bases, the aim of this study was to analyze two specific RAW-derived murine cell clones, namely, CRL-2278 and TIB-71 clones, which are iNOS-deficient and -proficient cell lines, respectively, in order to evaluate the role of NO release in modulating osteoclastic differentiation induced by M-CSF and RANKL.

MATERIALS AND METHODS

Cell Cultures and Treatments

As a model system of osteoclastogenesis, we have used two clones of RAW 264.7 murine monocytic/macrophagic cell line, purchased from American Type Culture Collection (ATCC, Rockville, MD). The first clone of RAW 264.7, the so-called TIB-71, is derived from a murine tumor induced by Abelson leukemia virus (A-MuLV). RAW 264.7 gamma NO (−) clone CRL-2278, instead, was derived from the TIB-71 clone and, unlike the parental line, does not produce nitric oxide upon treatment with interferon (IFN) or lipopolysaccharide (LPS) alone, but requires LPS plus IFN for full activation. TIB-71 cells were cultured in a 24-well plate at a density of 1×10^5 cells/mL in Dulbecco's modified Eagle's medium with 4 mM L-glutamine and modified to a final concentration of 4.5 g/L glucose, 1.5 g/L sodium bicarbonate, and 10% fetal bovine serum (FBS). CRL-2278 was cultured in a 24-well plate at a density of 1×10^5 cells/mL in RPMI-1640 medium with 2 mM L-glutamine and modified to a final concentration of 4.5 g/L glucose, 1.5 g/L sodium bicarbonate, 10 mM Hepes, 1 mM sodium piruvate, and 10% fetal bovine serum (FBS).

For osteoclastic differentiation, cells were cultured for 10 days in the presence of 10 ng/mL recombinant murine M-CSF (R&D, Minneapolis, MN) and 25 ng/mL human RANKL (Alexis, Lausen, Switzerland). The cytokine cocktail concentrations were determined after a set of preliminary experiments aimed at determining the best cocktail inducing osteoclastic differentiation in both cell lines (not shown). In selected experiments, cells were treated with the NO inhibitor N-nitro-L-arginine methyl ester hydrocloride (L-NAME; Sigma, St. Louis, MO) at a final concentration of 0.2 mM. Medium and treatments were replaced every 3 days. In experiments aimed at iNOS determination, cells were treated with LPS for full activation at a concentration of 10 ng/mL.

Morphological Analysis and Cytochemical Staining

To evaluate the cytokine-dependent morphological changes, cells were plated on glass slides, allowed to grow at confluence for 24 hr (day 0), then treated with cytokines for 10 days. Morphological changes of the cells were assessed at days 3, 7, and 10 by an inverted microscope and digitally with a Canon Power-Shot G3 Camera (Canon, Tokyo, Japan), RS Image, and Optimas 6 (Media Cybernetics, Washington, DC) software for image analysis.

For electron microscopy analysis, cells were grown in the same conditions as for optical microscopy. After a brief rinse in PBS, cells attached to a glass surface were fixed with 2% glutaraldehyde in 0.1 M phosphate buffer, pH 7.3, for 30 min at 4°C. Cells were then rinsed in 0.1 M phosphate buffer, pH 7.3, postfixed with 1% osmium tetroxide in the same buffer for 1 hr at 4°C, dehydrated in ascending alcohol, and treated with propylene oxide. After embedding in araldite (Electron Microscopy Sciences, Ft. Washington, PA), ultrathin sections of the cell monolayers were cut with a Reichter OM ultramicrotome. Sections were stained with uranyl-acetate and lead cytrate and then examined with a transmission electron microscope JEOL model 100S (JEOL, Peabody, MA).

Bone Resorption Assay

RAW 264.7 cells were plated on 24-well plates coated with artificial bone slides (OAAS; Osteogenic Core Technologies, Choongnam, Korea) and allowed to attach overnight. Cytokines were added starting from the next day. After 10 days, plates were processed according to the manufacturer's instruction, and resorption lacunae were visualized using a light microscope.

TRAP and NO Assays

For cytochemical tartrate-resistant acid phosphatase (TRAP) analysis, cells were stained using a leukocyte acid phosphatase kit according to the manufacturer's instruc-

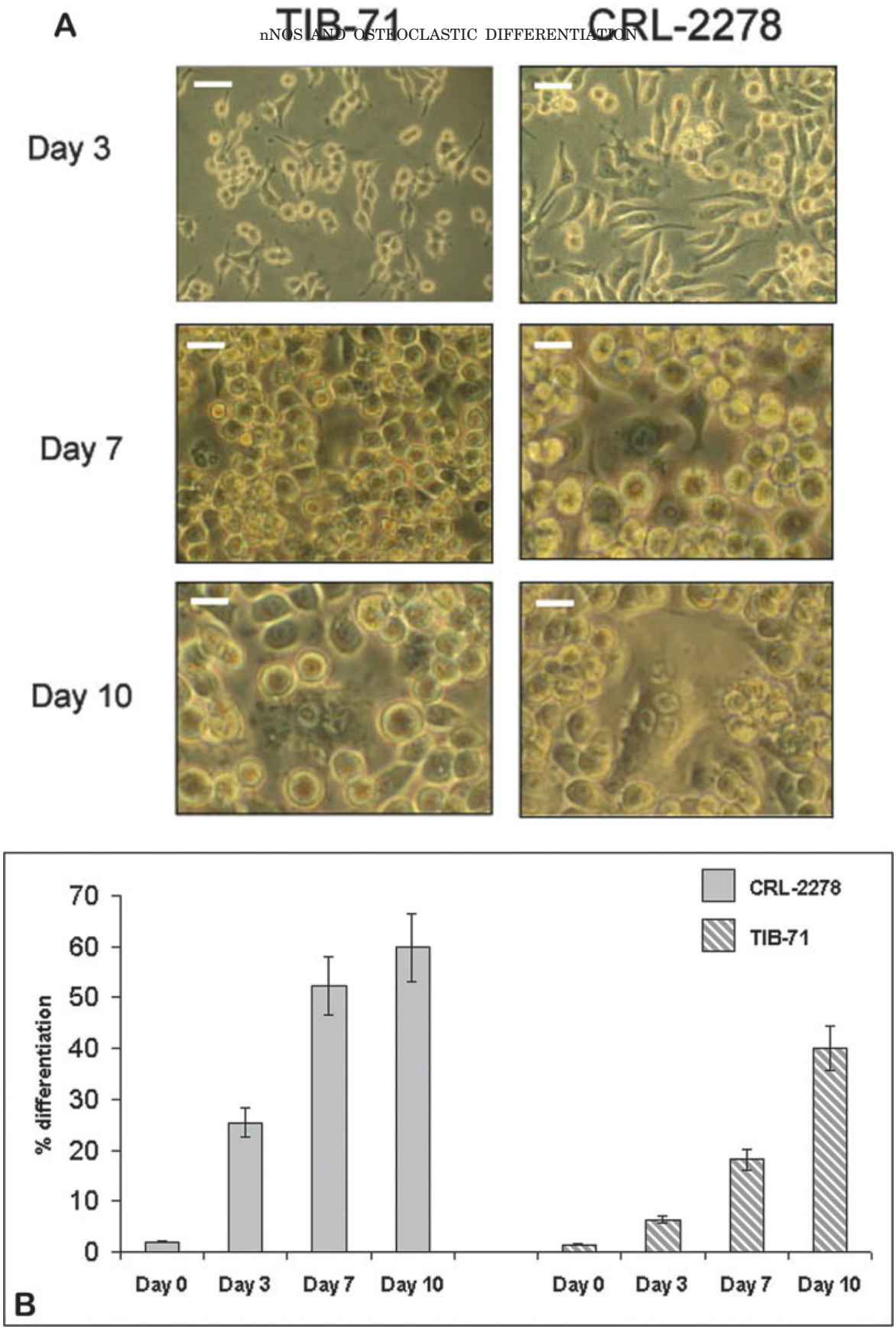

Fig. 1. **A:** Comparative morphological analysis of CRL-2278 and TIB-71 RAW clones at days 3, 7, and 10 of treatment with RANKL and M-CSF by optical microscopy. CRL-2278 cultures show the presence of polynucleated cells at day 7 of treatment onward, while TIB-71 clone only at day 10 of treatment. Scale bars = 25 μm (day 3 panels); 50 μm (day 7–10 panels:). **B:** Differentiation quantification of CRL-2278 and TIB-71 cell cultures. Figure shows percentage of in vivo polynucleated cells at inverted optical microscopy, obtained from CRL-2278 and TIB-71 clones treated with RANKL and M-CSF cocktail for 0–10 days. Filled bars, CRL-2278 clone; hatched bars, TIB-71 clone.

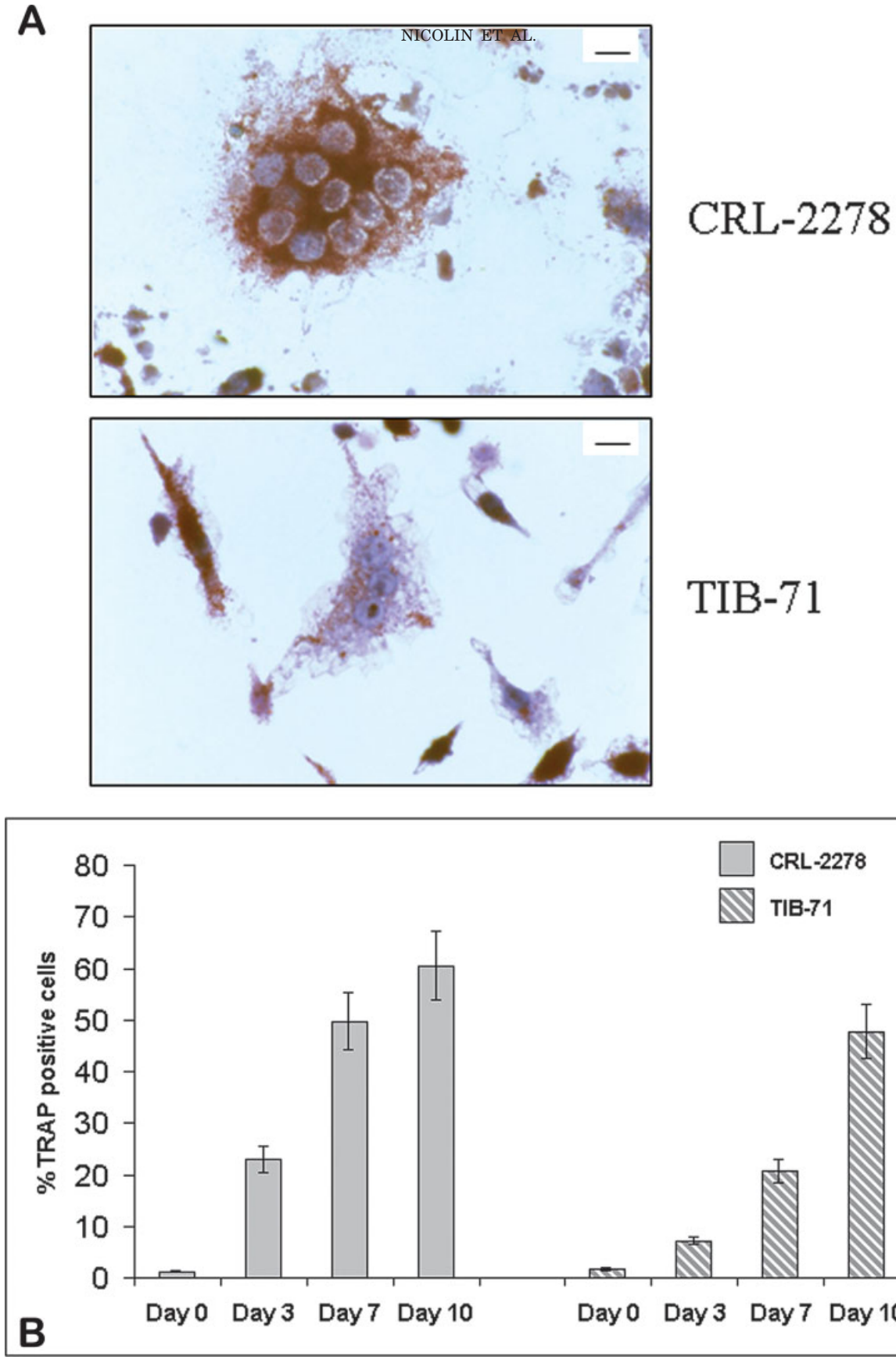

Fig. 2. **A:** TRAP assay. Figure shows TRAP positivity of polynucleated cells obtained after 10 days of treatment of CRL-2278 and TIB-71 clones with RANKL and M-CSF. CRL-2278 clone presents a higher number of nuclei and larger cytoplasmic volume corresponding to a more advanced differentiation stage compared to TIB-71 cells. Scale bars = 50 μm. **B:** Differentiation quantification of CRL-2278 and TIB-71 cell cultures. Figure shows percentage of TRAP-positive cells evaluated at light microscopy after treatment of CRL-2278 and TIB-71 clones with RANKL and M-CSF cocktail for 0–10 days. Filled bars, CRL-2278 clone; hatched bars, TIB-71 clone.

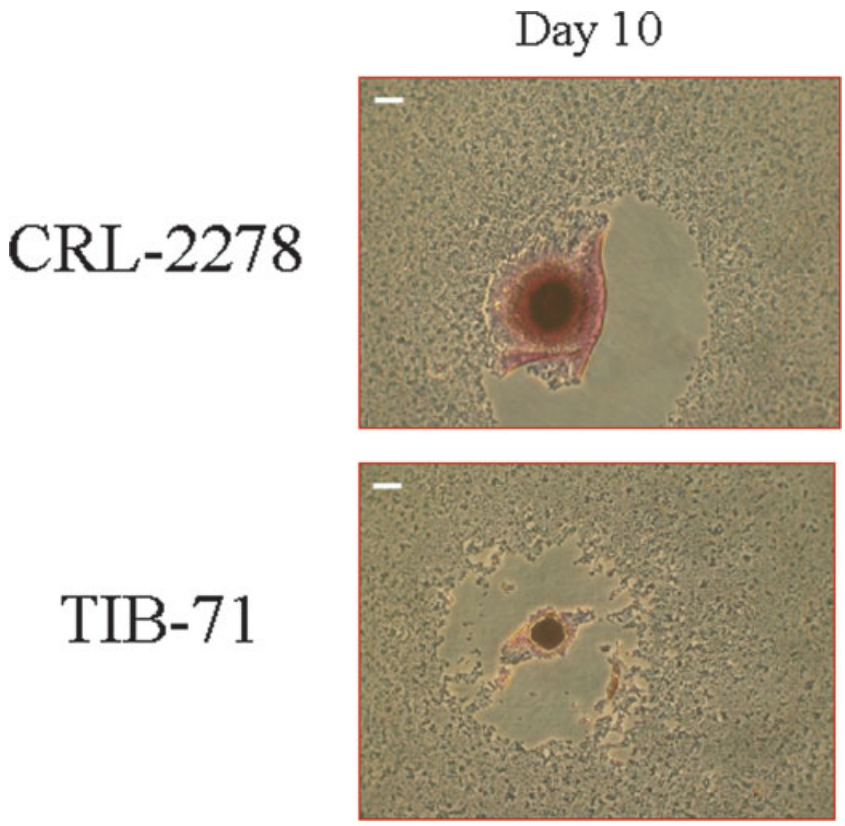

Fig. 3. Functional assay. Figure shows the effect of RANKL and M-CSF on functionality of differentiated CRL-2278 and TIB-71 clones. RAW clones were plated on an artificial bone matrix slide and were cultured with RANKL + M-CSF for 10 days. After 10 days, the slides were fixed and stained, and resorption was determined by examining pit formation under a light microscope (magnification, 20×).

tions (387-A; Sigma). Briefly, cells were washed once in PBS and fixed for 30 min in a solution of 4% paraformaldehyde. Fixed cells were then washed in PBS and incubated for 1 hr at 37°C in TRAP staining solution. After TRAP reaction, slides were rinsed in deionized water and counterstained with hematoxilin solution for 1–2 min, then dried on air and evaluated microscopically by a Phometrics Cool Snap (Roper Scientific, Duluth, GA). Cell culture NO activity was analyzed by nitric oxide (NO_2^-/NO_3^-) assay (R&D, Minneapolis, MN) following the manufacturer's instructions.

Cell Cycle Analysis

Samples containing 2–5 × 10^5 cells were harvested by centrifugation at 200 *g* for 10 min at 4°C, fixed with 70% cold ethanol for 1 hr at 4°C, and treated as previously described (Zauli et al., 1994). Analysis of PI fluorescence was performed by Argon laser-equipped FACScan flow cytometer with the FL2 detector in a linear mode using the Lysis II software (Becton Dickinson, San Jose, CA). Cell cycle analysis was carried out as described in Zauli et al. (1994).

Western Blot Analysis

Cells were harvested in lysis buffer containing 1% Triton X-100, Pefablock (1 mM), aprotinin (10 g/mL), pepstatin (1 g/mL), leupeptin (10 g/mL), NaF (10 mM), and Na_3VO_4 (1 mM) at specific times. Equal amounts of protein (40 μg/lane) were resolved by 12% sodium dodecyl sulfate-polyacrylamide gel electrophoresis and transferred onto a nitrocellulose membrane (Amersham, Little Chalfont, U.K.). The membrane was then washed with Tris-buffered saline (TBS; 10 mM Tris, 150 mM NaCl) containing 0.05% Tween 20 (TBST) and blocked in TBST containing 5% nonfat dried milk. The membrane was further incubated with the following antibodies: anti-iNOS, anti-eNOS, anti-nNOS (all diluted 1/2,000; Becton-Dickinson); anticyclin B1, anti-Cdc2 p34 (all diluted 1/2,000; Santa Cruz Biotechnology, Santa Cruz, CA); or antitubulin I (1/2,000; Sigma). The membrane was then incubated with appropriate secondary antibodies coupled to horseradish peroxidase (1/5,000; Sigma) and developed by ECL Western detection kit (Amersham).

Statistical Analysis

The results were evaluated by using analysis of variance with subsequent comparisons by Student's *t*-test for paired or nonpaired data as appropriate. Statistical significance was defined as $P < 0.05$. Values are reported as mean ± standard deviation (SD).

RESULTS

CRL-2278 Cells Show Faster and Stronger Osteoclastic Differentiation With Respect to TIB-71 Cells in Response to RANLK + M-CSF

In the first group of experiments, two different clones of RAW 264.7, namely, CRL-2278 and TIB-71, were treated with predetermined optimal concentrations of M-CSF (10 ng/ml) and RANKL (25 ng/ml). No differentiation was observed when cell treatment was carried out with RANKL or M-CSF used as single agents, clearly suggest-

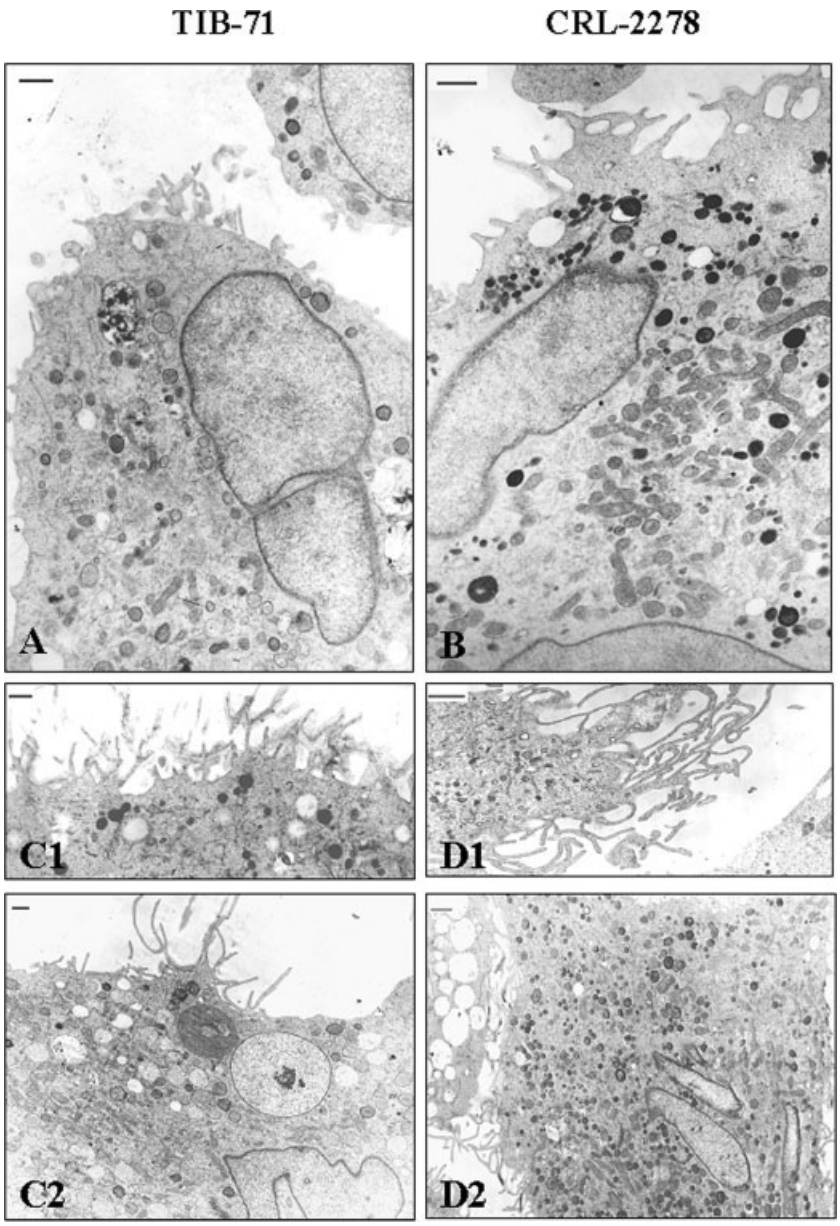

Fig. 4. Transmission electron microphotographies of TIB-71 and CRL-2278 RAW clones at different stages of differentiation. **A** and **B:** CRL-2278 and TIB-71 RAW clones at 7 days of treatment with RANKL and M-CSF. Both clones appear to be already binucleated; however, TIB-71 cells present a negligible development of ruffle border and a lower number of lisosomial vescicles if compared to CRL-2278 cells. **C1** and **C2:** TIB-71 RAW clone at 10 days of treatment with RANKL and M-CSF. TIB-71 cells show an initial development of ruffle border (short microvilli) and only a few cytoplasmic lisosomial vescicles. **D1** and **D2:** CRL-2278 RAW clone at 10 days of treatment with RANKL and M-CSF. CRL-2278 cells evidence a higher level of maturation of ruffle border, with much longer and convoluted microvilli and higher density of lisosomial vescicles. Scale bars = 1 μm.

ing that the combined activity of RANKL and M-CSF is needed to induce osteoclastic differentiation in these cell models (data not shown). Osteoclastic differentiation of CRL-2278 and TIB-71 cell clones was initially examined by light microscopy at different culture times (days 0, 3, 7, and 10 after treatment). Repeated experiments clearly demonstrated that CRL-2278 cells displayed morphological features of multinucleated osteoclasts, starting from day 3 and being clearly evident at day 7. On the other hand, morphological characteristics of osteoclastic differentiation were observed in TIB-71 cells only at day 10 of culture (Fig. 1). The degree of osteoclastic differentiation was also analyzed by TRAP staining on both RAW 264.7 cell clones in order to corroborate the morphological data (Fig. 2A). The percentage of positivity to TRAP, an early marker of osteoclastic differentiation, was significantly ($P < 0.05$) higher in CRL-2278 than in TIB-71 cells from day 3 onward, confirming that osteoclastic differentiation occurred earlier in CRL-2278 with respect to TIB-71 cells (Fig. 2B).

To evaluate whether the differences between the two RAW 264.7 clones were functional, the bone resorption activity was investigated using the OAAS oscotech system (Fig. 3). TEM analysis of both clones showed that at day 7 of treatment with RANKL and M-CSF cocktail (Fig. 4A and B), no essential differences can be evidenced in the development of the two clones, if not for the initial appearance of ruffle border in CRL-2278 cells. However, at day 10 of culture, CRL-2278 cells (Fig. 4D1 and D2) were larger than TIB-71 cells and showed a more evident ruffle border (Fig. 4C1 and C2). Moreover, the number of lacunae was significantly higher in CRL-2278 as compared to TIB-71

cells, clearly indicating that not only osteoclastogenesis was anticipated in CRL-2278 cells but that the number of functional osteoclasts was greater ($P < 0.05$) in the CRL-2278 cell clone.

RANKL- and M-CSF-Treated CRL-2278 Clone Shows Higher Percentage of Cells in S/G2-M Phase as Compared to TIB-71 Clone

To investigate whether the different rate in osteoclastic differentiation observed between CRL-2278 and TIB-71 cell clones was accompanied to differences in their cycling activity, we next compared cell cycle profile of both cell clones by flow cytometry analysis at different culture times. In parallel, the key cell cycle-related proteins were examined by Western blot. As shown in Table 1, cell cycle analysis of both clones treated or not with M-CSF + RANKL showed that the number of cells in the S/G2-M phase of the cell cycle was higher ($P < 0.05$) in CRL-2278 as compared to TIB-71. Consistent with the flow cytometry data, Western blot analysis showed that the expression of Cdc-2 and cyclin B1 proteins (Fig. 5), which are critically involved in S/G2-M progression, was higher in CRL-2278 cells, being detectable until 7–10 days after treatment. On the other hand, these proteins were barely detectable in TIB-71 cells at day 7 of culture and completely disappeared at day 10.

TABLE 1. Flow cytometry cell cycle analysis of CRL-2278 and TIB-71 RAW clones at days 0, 7, and 10 of treatment with RANKL and M-CSF

	Cell cycle analysis of differentiating RAW clones				
	% Apoptosis	G_0/G_1	S	G_2/M	
Day 0	1	95	2	2	TIB-71
Day 3	3	91	5	2	
Day 7	4	87	7	2	
Day 10	3	85	8	4	
Day 0	2	69	18	11	CRL-2278
Day 3	2	79	12	7	
Day 7	1	76	16	7	
Day 10	6	81	10	3	

CRL-2278 Cells Show Increased Basal Production and Nitric Oxide and Enhanced Expression of nNOS With Respect to TIB-71

Since nitric oxide production has been shown to be critically involved in modulating osteoclastic survival activity, we next investigated the pattern of NOS isoform expression and the nitric oxide production levels in the CRL-2278 and TIB-71 cell clone (Fig. 6). While nitric oxide production/release in culture supernatant was barely detectable in TIB-71 cells, CRL-2278 released significantly ($P < 0.05$) greater amounts (30-fold higher than TIB-71) at all culture time examined. In further experiments, the expression of iNOS, nNOS, and eNOS isoforms was examined by Western blot (Fig. 7). CRL-2278 showed significantly higher levels of expression of nNOS as compared to TIB-71 cell line. As expected, under LPS treatment, iNOS was expressed in TIB-71 cells but not in CRL-2278, while eNOS was undetectable under all culture conditions.

To ascertain whether the constitutive expression of nNOS was involved in the increased propensity of CRL-2278 to undergo osteoclastic differentiation as compared to TIB-71, CRL-2278 cells were treated with L-NAME, a broad NOS inhibitor. The addition in culture of L-NAME showed no significant toxicity on cell viability. Moreover,

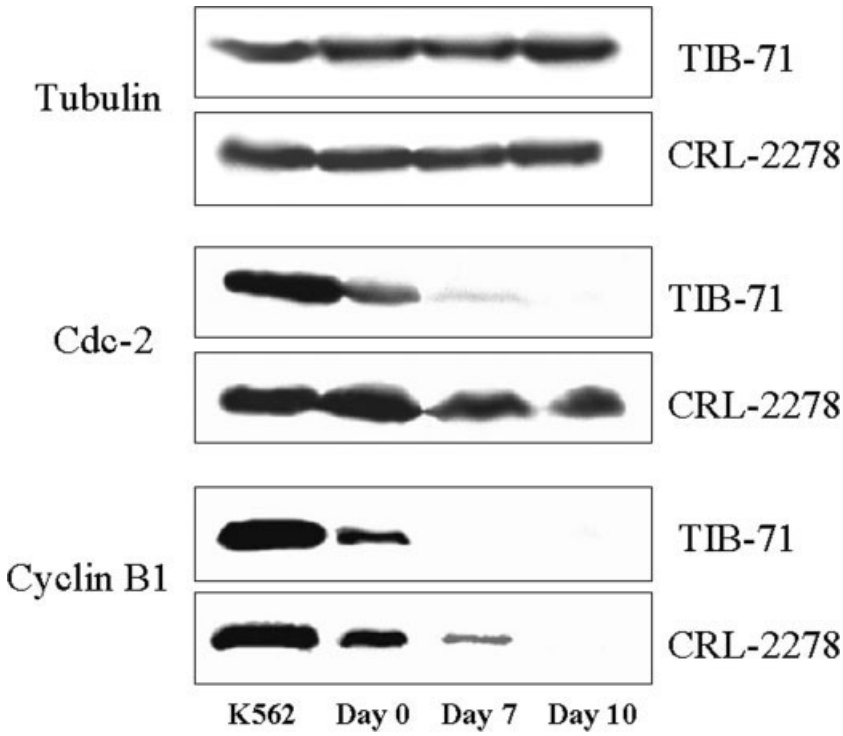

Fig. 5. Western blot analysis of Cdc-2 and cyclin B1 in CRL-2278 and TIB-71 RAW clones at days 0, 7, and 10 of treatment with RANKL and M-CSF. Positive control: K562 cell line lysate. Cdc-2 panel: at day 7 of treatment, Cdc-2 is hardly detectable in TIB-71 clones while well evident in CRL-2278 clone. Cyclin B1 panel: at day 7 of treatment, cyclin B1 is still detectable in CRL-2278 while completely downregulated in TIB-71 clone.

while L-NAME had no significant effect on TIB-71 clone osteoclastic differentiation, when added to CRL-2278 cells, it significantly ($P < 0.05$) reduced the percentage of TRAP-positive cells to levels comparable with TIB-71 clone (Fig. 8), clearly suggesting that nNOS-mediated basal production of nitric oxide was critically involved in enhancing osteoclastic differentiation in CRL-2278 cells.

DISCUSSION

The osteoclastic differentiation and activity plays a pivotal role in bone biology. This type of tissue is regulated by a large number of stimuli, even though cell differentiation is mainly controlled by two cytokines: RANKL and M-CSF. In this study, we have analyzed the osteoclastic differentiation of two specific cell clones (CRL-2278 and TIB-71) of RAW 264.7, a widely employed murine macrophage preosteoclast cell model. Particularly, CRL-2278 differs from parental TIB-71 cell line since it does not produce NO upon treatment with IFN or LPS used alone. NO is a pleiotropic signaling molecule with important regulatory effects on bone tissue development and homeostasis. NO is generated from L-arginine and molecular oxygen by the action of NOS. Three isoforms of NOS (types I, II, and III) have been identified: the neuronal (type I) and endothelial (type III) enzymes are constitutively expressed in several cells and thought to be involved in the basal regulation of cellular physiology and metabolism (Fox and Chow, 1998). The third member of the NOS family, iNOS (type II), is an inducible enzyme, initially identified in murine macrophages stimulated with bacterial LPS and/or IFN (van't Hof et al., 2000).

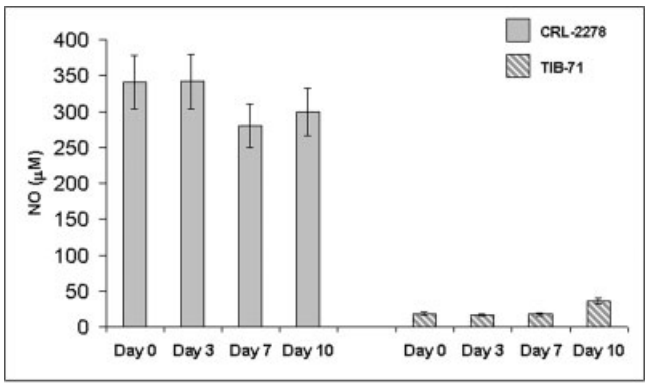

Fig. 6. Nitric oxide assay. NO production (μM) of CRL-2278 and TIB-71 clones at days 0, 7, and 10 of treatment with RANKL and M-CSF. CRL-2278 clone produces much high levels of NO when compared to TIB-71 clone at any time of treatment. NO production is independent by confluence conditions of cell cultures (not shown). Filled bars, RAW CRL-2278 clone; hatched bars, RAW TIB-71 clone.

We have here demonstrated that CRL-2278 cells undergo a quicker osteoclastic differentiation with respect to TIB-71 in the presence of RANKL and M-CSF. The increased osteoclastic differentiation of CRL-2278 cell line was also accompanied to a higher rate of cycling activity as compared to TIB-71. Moreover, in spite of the fact that CRL-2278 cells do not express iNOS in response to LPS, this cell clone showed a much higher basal constitutive NO release compared to TIB-71. Such high level of NO release by CRL-2278 was nNOS-dependent. In fact, CRL-2278 cells did not express either eNOS or iNOS, while they express nNOS at significantly higher levels than TIB-71. Moreover, the importance of nitric oxide production and release in accounting for the enhanced propensity to undergo osteoclastic differentiation of CRL-2278 with respect to TIB-71 was demonstrated by the ability of L-NAME, a broad inhibitor of NOS activity, to affect the

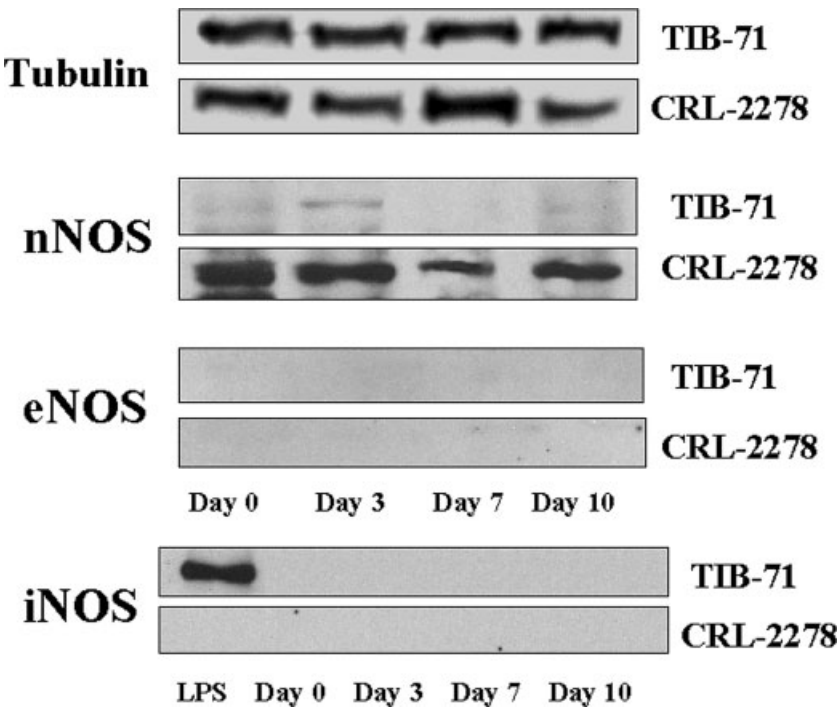

Fig. 7. Western blot analysis of NOS isoforms in CRL-2278 and TIB-71 RAW clones. nNOS is expressed at high levels in CRL-2278 clone while scarcely detectable in TIB-71 clone. eNOS is absent in both cell clones. iNOS is expressed under LPS activation only in TIB-71 clone.

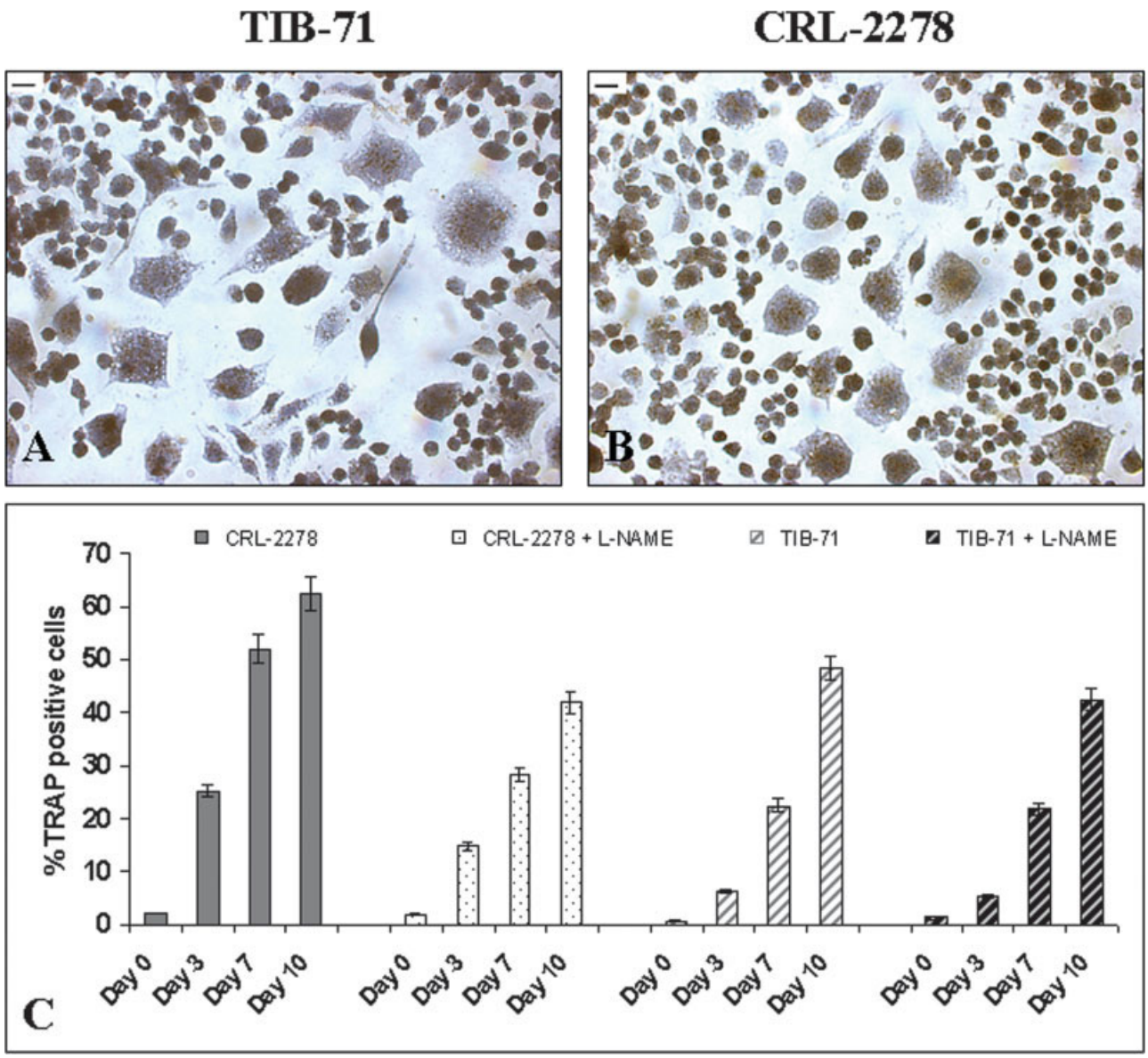

Fig. 8. Dependence of CRL-2278 and TIB-71 clone differentiation on NO levels. **A** and **B:** A representative of TRAP positivity of polynucleated cells at light microscopy, obtained after 10 days of treatment of CRL-2278 and TIB-71 clones, with RANKL and M-CSF ± NOS inhibitor L-NAME. Scale bars = 50 μm. **C:** Percentage of TRAP-positive cells after treatment of CRL-2278 and TIB-71 clones with RANKL and M-CSF ± NOS inhibitor L-NAME cocktail for 0–10 days of culture. Addition of L-NAME to cell cultures reduced CRL-2278 rate of differentiation to levels comparable with TIB-71 clones. L-NAME had no significant effect on TIB-71 rate of differentiation.

degree of osteoclastic differentiation in CRL-2278 significantly. Our results should be considered in the context of several previous studies, which have reported contrasting and sometimes opposite roles of the biological activity of NO in osteoclastogenesis, mainly depending on the cell model and experimental conditions employed (MacIntire, 1991; Kasten et al., 1994, Collin-Osdoby et al., 2000). In fact, pharmacological treatment with NO donors was able to reduce ovariectomy-induced bone loss in a rat model (Hukkanen et al., 2003), suggesting a negative role of NO on osteoclastogenesis. Moreover, deficient iNOS (van't Hof et al., 2000) mice showed an inhibition of osteoclastic functional activity, while eNOS knockout mice showed an impaired osteoblast function (Aguirre et al., 2001). Insufficient cellular NO concentration reduced consistently osteoclast differentiation from mouse bone marrow cells (Holliday et al., 1997), while other study reported that NO induced a reduction of osteoclast formation (van't Hof and Ralston, 1997). In order to get over these contradictions, some authors have recently proposed an interesting explanation of these studies suggesting that low-intermediate levels of NO induce osteoclast activity and survival while either the absence or the excess of NO inhibits osteoclast activation and survival (Brandi et al., 1995).

In keeping with this hypothesis, we have here demonstrated that a basal level of NO release significantly in-

crease osteoclastogenesis in the RAW murine cell model. In this respect, a study by van't Hof et al. (2004) evidences that nNOS knockout mice-derived bone marrow cultures increased osteoclast differentiation levels under RANKL and M-CSF stimulation in vitro, but not in vivo. These contrasting data evidence how different experimental model can deeply affect results regarding osteoclastogenesis efficiency, therefore suggesting that this cellular differentiation mechanism is likely to be finely tuned by different unidentified factors. Although other authors (Helfrich et al., 1997; Fox and Chow, 1998) failed to find expression of nNOS in osteoclasts, it should be considered that a great variability is often observed in different cell and animal models. In spite of these discrepancies, our study demonstrates that different levels of nNOS expression might account for the different ability of RAW macrophage clones to undergo osteoclastic differentiation. Our data are also in agreement with the findings reported in a recent study showing that knockout nNOS mice have impaired osteoclastogenesis (Jung et al., 2003) and suggesting that this impairment may be due to a decreased production of NO by preosteoclasts.

ACKNOWLEDGMENTS

The authors thank Mrs. Giovanna Baldini for her support in electron microscopy analyses and Professor Davide Gibellini for his kind help in cytofluorimetric assays.

LITERATURE CITED

Aguirre J, Buttery L, O'Shaughnessy M, Afzal F, Fernandez DM, Hukkannen M, MacIntyre I, Polak J. 2001. Endothelial nitric oxide synthase gene-deficient mice demonstrate marked retardation in postnatal bone formation, reduced bone volume, and defects in osteoblast maturation and activity. Am J Pathol 158:247–257.

Bab IA, Einhorn TA. 1994. Polypeptide factors regulating osteogenesis and bone marrow repair. J Cell Biochem 55:358–365.

Boyle WJ, Simonet WS, Lacey DL. 2003. Osteoclast differentiation and activation. Nature 423:337–342

Brandi ML, Hukkanen M, Umeda T, Moradi-Bidhendi N, Bianchi S, Gross SS, Polak JM, MacIntyre I. 1995. Bidirectional regulation of osteoclast function by nitric oxide isoforms. Proc Natl Acad Sci USA 92:2954–2958.

Collin-Osdoby P, Rothe L, Bekker S, Anderson F, Osdoby P. 2000. Decreased nitric oxide levels stimulate osteoclastogenesis and bone resorption both in vitro and in vivo on the chick chorioallantonic membrane in association with neoangiogenesis. J Bone Miner Res 15:474–488.

Cundy T, Hegde M, Naot D, Chong B, King A, Wallace R, Mulley J, Love DR, Seidel J, Fawkner M, Banovic T, Callon KE, Grey AB, Reid IR, Middleton-Hardie CA, Cornish J. 2002. A mutation in the gene TNFRSF11B encoding osteoprotegerin causes an idiopathic hyperphosphatasia phenotype. Hum Mol Genet 21:19–27.

Fox SW, Chow JW. 1998. Nitric oxide syntase expression in bone cells. Bone 23:1–6.

Helfrich MH, Evans DE, Grabowsky PS, Pollock JS, Oshima H, Ralston SH. 1997. Expression of nitric oxide syntase isoforms in bone and bone cell cultures. J Bone Miner Res 12:1108–1115.

Holliday LS, Dean AD, Lin RH, Greenwald JE, Gluck SL. 1997. NO concentrations inhibit osteoclast formation in mouse marrow cultures by cGMP-dependent mechanism. Am J Physiol 272:F283–F291.

Hukkanen M, Platts LA, Lawes T, Girgis SI, Konttinen YT, Goodship AE, MacIntyre I, Polak JM. 2003. Effect of nitric oxide donor nitroglycerin on bone mineral density in a rat model of estrogen deficiency-induced osteopenia. Bone 32:142–149.

Jung JY, Lin AC, Ramos LM, Faddis BT, Chole RA. 2003. Nitric oxide syntase I mediated osteoclast activity in vitro and in vivo. J Cell Biochem 89:613–621.

Kasten TP, Collin-Osdoby P, Patel N, Osdoby P, Krukowski M, Misko TP, Settle SL, Currie MG, Nickols GA. 1994. Potentiation of osteoclast bone-resorption activity by inhibition of nitric oxide synthase. Proc Natl Acad Sci USA 91:3569–3573.

Lee SE, Chung HB, Kwak CH, Chung KB, Kwack ZH. 2001. Tumor necrosis factor-alpha supports the survival of osteoclast through the activation of Akt and ERK. J Biol Chem 276:49343–49349.

Liu W, Xu D, Yang H, Xu H, Shi Z, Cao X, Takeshita S, Liu J, Teale M, Feng X. 2004. Functional identification of three receptor activator of NF-kappa B cytoplasmic motifs mediating osteoclast differentiation and function. J Biol Chem 279:54759–54769.

Lowik CW, Nibbering PH, van de Ruit M, Papapoulos SE. 1994. Inducible production of nitric oxide in osteoblast-like cells and in fetal mouse bone explants is associated with suppression of osteoclastic bone resorption. J Clin Invest 93:1465–1472.

MacIntyre I, Zaidi M, Alam AS, Datta HK, Moonga BS, Lidbury PS, Hecker M, Vane JR. 1991. Osteoclastic inhibition: an action of nitric oxide not mediated by cyclic GMP. Proc Natl Acad Sci USA 88: 2936–2940.

Ralston SH, Ho LP, Helfrich MH, Grabowski PS, Johnston PW, Benjamin N. 1995, Nitric oxide: a cytokine-induced regulator of bone resorption, J Bone Miner Res 10:1040–1049.

van't Hof RJ, Ralston SH. 1997. Cytokine-induced nitric oxide inhibits bone resorption by inducing apoptosis of osteoclast progenitors and suppressing osteoclast activity. J Bone Miner Res 12:1797–1804.

van't Hof RJ, Armour KJ, Smith LM, Armour KE, Wei XQ, Liew FY, Ralston SH. 2000. Requirement of the inducible nitric oxide pathway for IL-1-induced osteoclastic bone resorption. Proc Natl Acad Sci USA 97:7993–7998.

van't Hof RJ, Macphee J, Libouban H, Helfrich MH, Ralston SH. 2004. Regulation of bone mass and bone turnover by neuronal nitric oxide synthase. Endocrinology 145:5068–5074.

Walsh MC, Choi Y. 2003. Biology of the TRANCE axis. Cytokine Growth Factor Rev 14:251–263.

Ye H, Arron JR, Lamothe B, Cirilli M, Kobayashi T, Shevde NK, Segal D, Dzivenu OK, Vologodskaia M, Yim M, Du K, Singh S, Pike JW, Darnay BG, Choi Y, Wu H. 2002. Distinct molecular mechanism for initiating TRAF6 signalling. Nature 25:443–447.

Zauli G, Vitale M, Re MC, Furlini G, Zamai L, Falcieri E, Gibellini D, Visani G, Davis BR, Capitani S. 1994. In vitro exposure to human immunodeficiency virus type 1 induces apoptotic cell death of the factor-dependent TF-1 hematopoietic cell line. Blood 83:167–175.

Zauli G, Rimondi E, Nicolin V, Melloni E, Celeghini C, Secchiero P. 2004. TNF-related apoptosis-inducing ligand (TRAIL) blocks osteoclastic differentiation induced by RANKL plus M-CSF. Blood 104: 2044–2050.